

Study of Intensification Zones in a Rectangular Acoustic Cavity

Linda F. Peretti* and Earl H. Dowell†
Duke University, Durham, North Carolina 27706

The interior acoustic field of a rectangular acoustic cavity, which is excited by the structural vibration of one of its walls, or a portion of the wall, has been studied. Particularly, the spatial variations of sound pressure levels from the peak levels at the boundaries (intensification zones) to the uniform interior are considered. Analytical expressions, which describe the intensification zones, are obtained using the methodology of asymptotic modal analysis. These results agree well with results computed by a discrete summation over all of the modes. The intensification zones were also modeled as a set of oblique waves incident upon a surface. The result for a rigid surface agrees with the asymptotic modal analysis result. In the presence of an absorptive surface, the character of the intensification zone is dramatically changed. The behavior of the acoustic field near an absorptive wall is described by an expression containing the rigid wall result plus additional terms containing impedance information. The important parameter in the intensification zone analysis is the bandwidth to center frequency ratio. The effect of bandwidth is separated from that of center frequency by expanding the expression about the center frequency wave number. The contribution from the bandwidth is second order in bandwidth to center frequency ratio.

Nomenclature

A	= area
c	= speed of sound
F	= cavity acoustic modal function
f	= frequency
k	= wave number
L	= cavity dimension
M	= generalized mass
n	= modal index
p	= pressure
r_b	= real part of impedance
V	= volume
w	= displacement
x, y, z	= spatial position coordinates
x_b	= imaginary part of impedance
z_b	= impedance at the boundary
ΔN	= number of acoustic modes
ζ	= damping ratio
ρ	= density
Φ	= power spectrum
ω	= frequency
$\langle \rangle$	= spatially averaged quantity

Subscripts

b	= bandwidth
c	= center frequency
f	= flexible
o	= reference value
r	= acoustic modal index

Superscripts

A	= acoustic
\cdot	= time derivative
$-$	= (overbar on pressure) rms
$-$	= (overbar on impedance quantities) nondimensionalized by ρc

Introduction

IN structural-acoustic coupled systems, such as the interior of an automobile or an aircraft fuselage, an acoustic field is created by the structural vibration of a wall or walls of the enclosure. This problem has been studied previously using asymptotic modal analysis (AMA) on a rectangular acoustic cavity.^{1,2} The cavity was assumed to be entirely rigid except for a vibrating portion of one of its walls. The vibrating portion contained a large number of structural modes, which in turn generated a large number of acoustic modes in the interior space. Acoustic theory predicts, and the previous numerical work has shown, that there are intensification zones in the acoustic field near the cavity boundary and an otherwise uniform response in the interior region. This is due to the lack of spatial correlation in the interior and the imposition of spatial correlation at the boundaries. For a rectangular acoustic cavity, it is well known that the mean square pressures are eight, four, and two times the uniform interior pressure levels at the corners, edges, and faces, respectively.³⁻⁵

In designing acoustic spaces, allowances must be made for these intensification zones. Therefore, it is important to determine the characteristic distance over which the response levels change from their peak values at the boundary to the uniform interior level. If the distance from a boundary is nondimensionalized by the center frequency wave number k_c , then the intensification zone can be described by the nondimensionalized spatial variable $k_c x$ and the bandwidth to center frequency ratio f_b/f_c . Significantly, the parametric dependence is independent of cavity dimensions. The spatial variation of mean-square pressure is also independent of cavity dimensions. The spatial variation of mean-square pressure is also independent of the size of vibrating or absorptive surfaces on the cavity wall, provided that the surfaces are very large compared to an acoustic wavelength (high-frequency limit) and provided that the damping is small.

The dependence on bandwidth can be separated mathematically from the dependence on center frequency through a Taylor series expansion in f_b/f_c taken about the center frequency wave number. It is found that the bandwidth dependence is a higher order effect. The resulting mathematical expression for mean-square pressure consists of a term that is dependent only on the center frequency, plus terms that contain the bandwidth to center frequency ratio; but these terms are of order $O[(f_b/f_c)^2]$ and higher.

Received March 11, 1991; revision received July 8, 1991; accepted for publication March 9, 1991. Copyright © 1991 by the American Institute of Aeronautics and Astronautics, Inc. All rights reserved.

*Research Assistant Professor, Department of Mechanical Engineering and Materials Science, School of Engineering.

†Dean and Professor, Department of Mechanical Engineering and Materials Science, School of Engineering.

Using AMA, the spatial variation of mean-square pressure was found to be independent of cavity dimensions. This suggests that the problem can also be analyzed as a local problem consisting of an infinite number of oblique acoustic waves incident upon a rigid surface from all possible angles. The solution to that problem is equivalent to that derived from AMA.

In the same manner, an expression can be obtained for the spatial variation of mean-square pressure, which describes the intensification zone near a boundary for a case where the incident wall is nonrigid (i.e., finite impedance cases). This result can be written in terms of a hard wall component plus an absorption correction term, which contains the impedance information.

The purpose of this research is to determine the structure of these intensification zones and their relation to the entire acoustic field. It is hoped that this work will lead to better design and analysis of acoustic spaces by providing a more thorough understanding of intensification zones for both rigid and absorptive walls.

Background

Intensification zones for structures have been studied extensively by Crandall⁶ and others for random vibrations of plates (see, e.g., Refs. 6–8). They have found that the response of the plate at high frequency is relatively uniform, with exceptions occurring at the point of application of a force and/or at the boundaries, depending on loading conditions and boundary conditions. Kubota and Dowell⁹ found similar intensification phenomena for a rectangular plate excited by random vibration of a point force. They used AMA to predict the response of the plate, and they verified their results with experimental data.

The study of intensification zones in acoustic spaces was first begun by Waterhouse¹⁰ in the 1950s. His pioneering work on interference patterns in reverberant sound fields was followed by further research by Chu,^{11,12} Tohyama and Suzuki,¹³ and others^{14,15} who were specifically interested in the placement of microphones in reverberation chambers. The results presented here for rigid wall boundaries agree with the earlier work, although the derivations are different. References 10–15 were restricted to rigid walls only. Later work by Waterhouse and Cook¹⁶ included the treatment of pressure release ($p = 0$) boundary conditions.

Parameterization of Intensification Zone

Asymptotic Modal Analysis Approach

A rectangular acoustic cavity with five rigid walls and one vibrating wall has been studied previously using AMA. A diagram of this problem is shown in Fig. 1. The vibrating wall was driven by white noise such that a large number of structural modes was excited in a particular bandwidth. It was assumed that a large number (approaching infinity) of acoustic modes was present in the interior acoustic cavity, and that these modes were temporally uncorrelated. Although it is not assumed in the AMA derivation, a consequence of the previous assumptions is that the acoustic modes are spatially uncorrelated as well. From Refs. 1 and 2, the expression for the mean-square pressure for a finite number of acoustic modes and an infinite number of structural modes is

$$\frac{\bar{p}^2}{(\rho_0 c_0^2)^2} \cong \frac{\pi}{4} \frac{A_f}{V^2} \Phi_w(\omega_c) \sum_r \frac{F_r^2(x, y, z)}{(M_r^A)^2 (\omega_r^A)^3 \zeta_r^A} \times \iint_{A_f} F_r^2(x, y, z_0) dx dy \quad (1)$$

As in AMA, M_r^A and ζ_r^A can be treated as constant in a band and can therefore be evaluated at the center frequency. Thus, for example, M_r^A becomes M_c^A , etc. Normalizing \bar{p}^2 by the spatially averaged \bar{p}^2 yields the following expression for the

nondimensionalized mean-square pressure in the rigid cavity with one entire wall flexible and vibrating:

$$\frac{\bar{p}^2}{\langle \bar{p}^2 \rangle} \cong \frac{\sum_r F_r^2(x, y, z) / (\omega_r^A)^3}{\sum_r \langle F_r^2(x, y, z) \rangle / (\omega_r^A)^3} \quad (2)$$

where the quantities in $\langle \rangle$ are spatially averaged values. This is the expression that describes the intensification zone near a boundary; it is a ratio of the local mean-square pressure to the spatially averaged (or uniform interior value) mean-square pressure. At interior points, this ratio will asymptotically (for $r \rightarrow \infty$) approach 1.0, whereas at the boundaries, the ratio will be 2.0, 4.0, or 8.0 for walls, edges, or corners, respectively. There are several possible transitions to study: from a corner to an edge, a wall, or the interior; from an edge to a wall or the interior; and from a wall to the interior. For each case, there are one-, two-, and three-dimensional modes to consider.

For the rectangular acoustic cavity, Dowell et al.¹⁷ have shown that hard-box modes can be used to describe the interior acoustic field, even when all six walls are not rigid. Therefore,

$$F_r^2(x, y, z) = \cos^2\left(\frac{n_x \pi x}{L_x}\right) \cos^2\left(\frac{n_y \pi y}{L_y}\right) \cos^2\left(\frac{n_z \pi z}{L_z}\right)$$

$$(\omega_r^A)^2 = \left(\frac{n_x \pi c}{L_x}\right)^2 + \left(\frac{n_y \pi c}{L_y}\right)^2 + \left(\frac{n_z \pi c}{L_z}\right)^2$$

One-Dimensional

Considering one-dimensional modes only, $F_r = \cos(n\pi x/L_x)$ and $\omega_r^A = n\pi c/L_x$. Assuming there are a large number of acoustic modes, which is consistent with the AMA approach, the discrete variable n can be treated as a continuous variable. Equation (2) becomes,

$$\frac{\bar{p}^2}{\langle \bar{p}^2 \rangle} \cong \frac{\int_n \cos^2\left(\frac{n\pi x}{L_x}\right) n^3 dn}{\frac{1}{2} \int_n 1/n^3 dn} \quad (3)$$

This integration can be done analytically, and the result is,

$$1 + \frac{f_c^2}{f_u^2 - f_l^2} \left\{ \frac{f_c^2}{f_l^2} \cos \theta_l - \frac{f_c^2}{f_u^2} \cos \theta_u + \frac{4\pi x f_c}{c} \right. \\ \times \left(\frac{f_c}{f_u} \sin \theta_u - \frac{f_c}{f_l} \sin \theta_l \right) + \left(\frac{4\pi x f_c}{c} \right)^2 [Ci(\theta_u) - Ci(\theta_l)] \left. \right\} \quad (4)$$

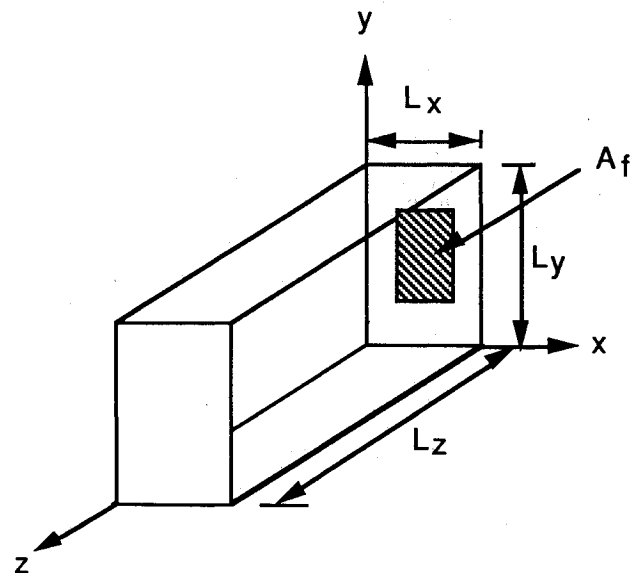


Fig. 1 Rectangular acoustic cavity that was studied.

1-D Intensification Summation Vs. Integration

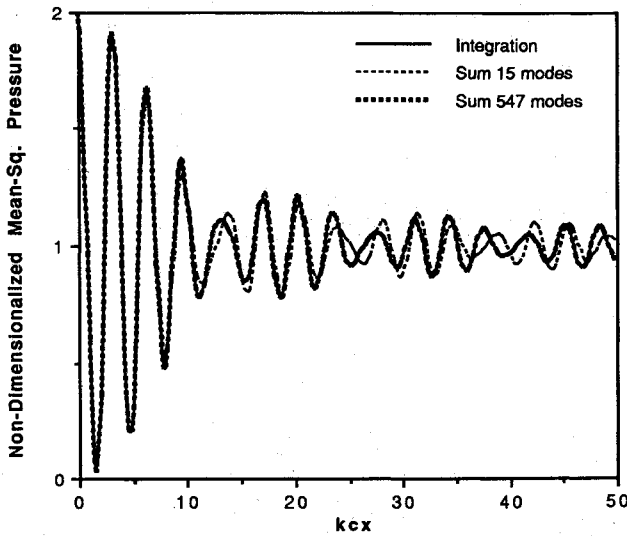


Fig. 2 Nondimensionalized mean-square pressure vs $k_c x$ computed three ways: as an integration in wave-number space, as a summation over 15 modes, and as a summation over 567 modes.

where f_c is the center frequency, f_b the frequency bandwidth, and f_l and f_u are defined as the lower and upper frequencies, respectively, of the frequency interval as follows: $f_u - f_l = f_b$, and $f_c = \sqrt{f_u \cdot f_l}$. The arguments of the cosines and the cosine integral function Ci are defined by $\theta_l = 2\pi k_c x f_l / f_c$, $\theta_u = 2\pi k_c x f_u / f_c$, where the nondimensional distance $k_c x$ is equal to $(2\pi f_c) x / c$.

The ratios f_l / f_c and f_u / f_c can be obtained from f_b / f_c using these definitions. In fact, the entire expression (8) can be written in terms of f_b / f_c and $k_c x$, where $k_c x$ is the product of the wave number associated with the center frequency and the distance from the endpoint. Knowing the ratio of frequency bandwidth to center frequency (f_b / f_c) allows the pressure function in the transition zone to be plotted as a function of nondimensionalized distance $k_c x$ away from the endpoint. Note that the dimensions of the cavity do not appear in this result.

If we assume that the frequency is approximately constant over the interval, and allow ω to equal ω_c , the result would be

$$\frac{\bar{p}^2}{\langle \bar{p}^2 \rangle} \cong 1 + \frac{1}{2} \frac{1}{(k_c x)(f_b / f_c)} \{ \sin(\theta_u) - \sin(\theta_l) \} \quad (5)$$

This is a decaying function that beats with some predictable frequency, as is shown in Fig. 2. In Fig. 2, both the previous approximation (5) and the discrete sum are plotted. The summation is performed for two different center frequencies, one in which 15 modes are present and the other in which 567 modes are present. The summation expression requires an additional parameter that is dependent on cavity dimension. Although the AMA (integration) approximation is theoretically valid when there are a large number of modes, here the approximation works well for relatively few modes. However, the agreement is not as good in the two- and three-dimensional cases.

Two-Dimensional Case

The transition zone for the two-dimensional case is slightly more complicated. In this case, $F_r = \cos(n\pi x / L_x) \cos(m\pi y /$

$L_y)$ and $(\omega_r^2)^2 = c^2[(n\pi x / L_x)^2 + (m\pi y / L_y)^2]$. Assuming there are a sufficiently large number of modes, m and n can be treated as continuous variables and the summation can be replaced by integration. Converting to wave-number space ($n\pi x / L_x = k_x$, etc.) and transferring k_x and k_y into polar coordinates by the relations $k_x = k \cos \alpha$ and $k_y = k \sin \alpha$, Eq. (2) can be written for the two-dimensional case as,

$$\frac{\bar{p}^2}{\langle \bar{p}^2 \rangle} = \frac{\int_0^{\pi/2} \int_0^{\pi/2} [\cos^2(kx \cos \alpha)][\cos^2(ky \sin \alpha)] / k^2 d\alpha dk}{\frac{1}{4} \int_0^{\pi/2} \int_0^{\pi/2} \frac{1}{k^2} d\alpha dk} \quad (6)$$

To show that this integral is dependent only on $k_c x$ and f_b / f_c , let $\xi = kx$. Then $ky = \xi y / x$ and $d\xi = x dk$. The nondimensionalized pressure ratio becomes

$$\frac{\bar{p}^2}{\langle \bar{p}^2 \rangle} \cong \frac{\int_{(k_l/k_c)k_c x}^{(k_u/k_c)k_c x} \int_{(k_l/k_c)k_c x}^{(k_u/k_c)k_c x} [\cos^2(\xi \cos \alpha)][\cos^2(\xi y / x \sin \alpha)] / \xi^2 d\xi d\alpha}{\int_{(k_l/k_c)k_c x}^{(k_u/k_c)k_c x} \int_{(k_l/k_c)k_c x}^{(k_u/k_c)k_c x} \frac{1}{\xi^2} d\xi d\alpha} \quad (7)$$

In Eq. (7), the only independent parameters are $k_c x$ and the ratios k_u / k_c and k_l / k_c , which can be derived from f_b / f_c . The ratio y / x is known from the desired location within the cavity. The geometry of the cavity itself (i.e., the cavity dimensions) is not an important parameter in determining the nondimensionalized pressure ratio of the cavity interior.

If we assume that k is a constant (i.e., $\Delta k / k \ll 1$), this expression can be integrated explicitly with the result that

$$\begin{aligned} \frac{\bar{p}^2}{\langle \bar{p}^2 \rangle} \cong & 1 + J_0(2k_c x) + J_0(2k_c y) + J_0(2k_c x) \cdot J_0(2k_c y) \\ & + \frac{8}{\pi} \sum_{m=1}^{\infty} \sum_{n=1}^{\infty} (-1)^n J_{2n}(2k_c x) J_{2m}(2k_c y) \\ & \times \left\{ \frac{\sin(m-n)\pi/2}{2(m-n)} + \frac{\sin(m+n)\pi/2}{2(m+n)} m \neq n \right. \\ & \left. (\pi/4) \quad m = n \right\} \end{aligned}$$

Notice in the limit as $k_c x$ and $k_c y$ asymptotically approach infinity, the Bessel functions decay and the nondimensionalized pressure ratio asymptotically approaches 1, whereas the k_c and $k_c y$ approach zero (i.e., near the corner), the higher-order Bessel functions decay, but $J_0(0) = 1$ and so the nondimensionalized pressure ratio asymptotically approaches 4.

Three-Dimensional Case

For the three-dimensional case, $F_r = \cos(n\pi x / L_x) \cos(m\pi y / L_y) \cos(\ell\pi z / L_z)$ and $\omega_r^2 = c^2[(n\pi / L_x)^2 + (m\pi / L_y)^2 + (\ell\pi / L_z)^2]$. Substituting these expressions into Eq. (2), making the appropriate assumptions to allow the summation to be replaced by integration (large number of modes, etc.), and transforming from modal index space to wave-number space yields the following expression in spherical wave-number coordinates:

$$\frac{\bar{p}^2}{\langle \bar{p}^2 \rangle} \cong \frac{8 \int \int \int_{k, \phi, \theta} [\cos^2(kx \sin \theta \cos \phi) \cdot \cos^2(ky \sin \theta \sin \phi) \cdot \cos^2(kz \cos \theta)] / k^3 \sin \theta d\theta d\phi dk}{\int \int \int_{k, \phi, \theta} (1/k^3) \sin \theta d\theta d\phi dk} \quad (8)$$

1-D Intensification Curves

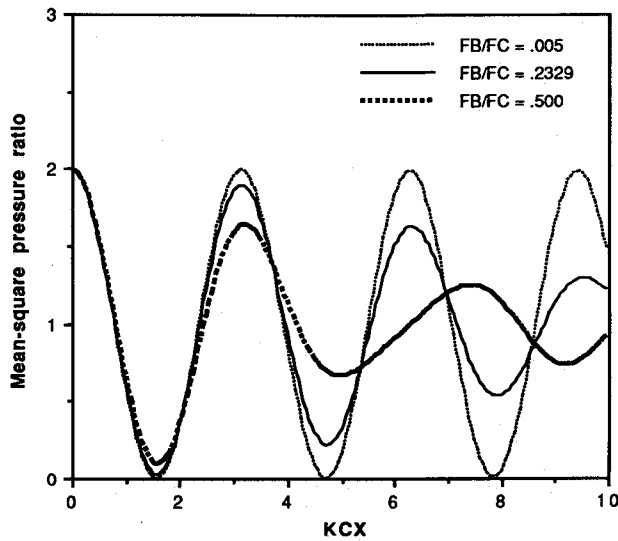


Fig. 3 Nondimensionalized mean-square pressure vs $k_c x$, one-dimensional case, three f_b/f_c ratios plotted: $f_b/f_c = 0.005, 0.23$, and 0.50 .

2-D Intensification Curves

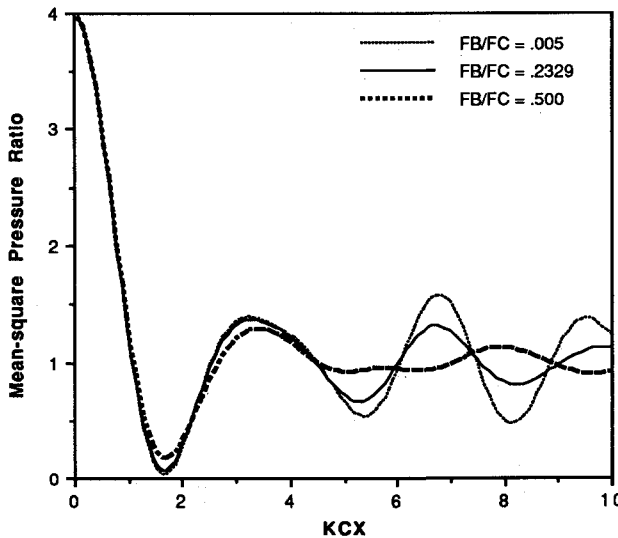


Fig. 4 Nondimensionalized mean-square pressure vs $k_c x$, two-dimensional case, three f_b/f_c ratios plotted: $f_b/f_c = 0.005, 0.23$, and 0.50 .

Again, it can be shown that the nondimensional pressure ratio is independent of cavity geometry and is, in fact, only dependent on the parameters $k_c x$, y/x , z/x , and f_b/f_c by performing a change of variables, as in the two-dimensional case. When the spatial variables are nondimensionalized by wave number, the transition zone can be plotted as a function of mean-square pressure vs position if the bandwidth to center frequency ratio is specified.

As the number of dimensions increases, the ratio f_b/f_c plays a less significant role in the shape of the transition zone, as can be seen upon comparison of Figs. 3-5. In each of the three figures, curves corresponding to three different f_b/f_c ratios are overlaid. The three f_b/f_c ratios are $f_b/f_c = 0.005$ (which corresponds to a narrow bandwidth at a high center frequency), $f_b/f_c = 0.23$ (corresponding to a $1/3$ octave band), and $f_b/f_c = 0.500$ (which corresponds to an octave band). For the one-dimensional case, Fig. 3 shows three distinct curves for the three different ratios. In the two-dimensional case, the three sepa-

rate curves are beginning to converge (Fig. 4), whereas in the three-dimensional case (Fig. 5), convergence occurs more rapidly. This trend is due to the large number of two- and three-dimensional modes for a given center frequency at fixed bandwidth.

Oblique-Wave Approach

Alternatively, the problem of intensification near boundaries can be analyzed as a local problem. At the walls, for example, the problem can be modeled as an infinite number of sound waves incident upon a rigid surface from infinitely many directions. The expression for the pressure at a point in the x, y plane due to a single sound wave, as shown in Fig. 6, is $p(x, y, t) = P e^{i(\omega t - k_x x - k_y y)}$, where $P = 2A \cos k_x x$, and A is the amplitude of the incident pressure wave. Assuming equal amplitude incident waves with random phase and random incidence angles (all equally probable), the summation of the mean-square pressures is

$$\sum_{\Delta\omega, \theta} \bar{p}^2 = \sum_{\Delta k, \theta} 2A^2 \cos^2(kx \cos \theta)$$

where k_x has been replaced by $k \cos \theta$.

Assuming there are a large number of frequencies in a particular bandwidth, as in AMA, the mean-square pressure in the band is

$$\bar{p}^2 = \int_{-\pi/2}^{\pi/2} 2A^2 \int_{k_{\text{lower}}}^{k_{\text{upper}}} \cos^2(kx \cos \theta) dk d\theta$$

3-D Intensification Curves

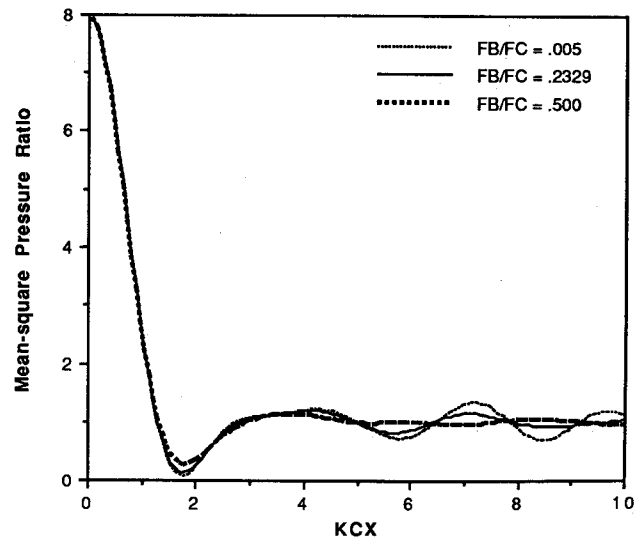


Fig. 5 Nondimensionalized mean-square pressure vs $k_c x$, three-dimensional case, three f_b/f_c ratios plotted: $f_b/f_c = 0.005, 0.23$, and 0.50 .

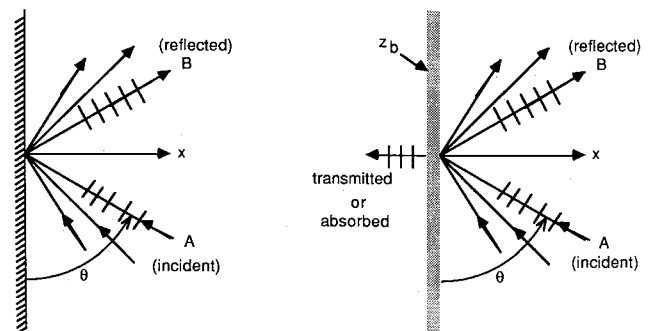


Fig. 6 Reflection from a rigid surface (left) or from an absorptive surface (right).

In order to compare this result to the AMA result, it must be nondimensionalized by its asymptotic far-field value (i.e., large $k_c x$), which is $2\pi A^2 (k_y - k_1)$. The corresponding result derived from AMA is Eq. (6). However, Eq. (6) contains variation in both the y and x directions. The nondimensionalized mean-square pressure ratio is equivalent to Eq. (6) for the two-dimensional AMA intensification from a wall providing that the y variable is held constant and the wave number is assumed large, such that the product ky approaches infinity. Note that the $1/k^2$ terms in Eq. (6) are contained in the pressure amplitude P for the oblique waves. These results also agree with the earlier result of Waterhouse¹⁰ which was derived using methods similar to the oblique-wave formulation.

Similar relations can be derived for the two- and three-dimensional incident sound fields with reflections from one, two, or three rigid surfaces. The methodology is similar to that presented here, and the results are in agreement with the AMA results.

Absorptive Wall Intensification

Using the oblique-wave approach outlined earlier, the effect of an absorptive wall can also be analyzed. Assume that an infinite number of oblique waves are incident upon an absorptive surface (of finite impedance, z_b) from infinitely many directions. Figure 6 shows one such pressure wave. The expression for the pressure from one wave is

$$p = P e^{i(\omega t - k_y y)} = 2A \left\{ \cos k_x x - \frac{e^{-ik_x x}}{\bar{r}_b \cos \theta + 1} \right\} e^{i(\omega t - k_y y)}$$

and

$$\bar{z}_b = z_b / \rho_0 c$$

Rewriting, $p = |P| e^{i(\omega t - k_y y + \phi_p)}$, where $P = |P| e^{i\phi_p}$. Then $p_{\text{real}} = |P| \cos(\omega t - k_y y + \phi_p)$. The mean-square pressure is equal to

$$\bar{p}^2 = \sum_{j=1}^{\text{No. of waves}} \frac{|P_j|^2}{2}$$

As in the previous analysis, assume that there are a large number of modes and replace the summation with integration. For equal amplitude waves, the expression for the mean-square pressure is

$$\bar{p}^2 = 2|A|^2 \int_{-\pi/2}^{\pi/2} \left\{ \cos^2(k_c x \cos \theta) - 2 \cos(k_c x \cos \theta) \left[\frac{(\bar{r}_b \cos \theta + 1) \cos(k_c x \cos \theta) - \bar{x}_b \cos \theta \sin(k_c x \cos \theta)}{(\bar{r}_b \cos \theta + 1)^2 + (\bar{x}_b \cos \theta)^2} \right] + \frac{1}{(\bar{r}_b \cos \theta + 1)^2 + (\bar{x}_b \cos \theta)^2} \right\} d\theta$$

Consistent with the assumptions of AMA, the wave number has been replaced by its value at the center frequency, assuming a narrow band with many modes. The first term in the expression is the same as in the rigid wall case. The far-field value (i.e., the limit for large $k_c x$) is

$$\bar{p}^2 = 2|A|^2 \int_{-\pi/2}^{\pi/2} \left\{ 1 - \frac{\bar{r}_b \cos \theta}{(\bar{r}_b \cos \theta + 1)^2 + (\bar{x}_b \cos \theta)^2} \right\} d\theta$$

After dividing by the expression for the far-field mean-square pressure, the end result is an expression that is equivalent to the rigid wall mean-square pressure result, but with a set of terms added to include the effects of absorption.

These expressions can be extended to three dimensions by integrating in spherical coordinates around both angular directions. If desired, inclusion of the bandwidth effect is also

Absorption Results: 2000 Hz Center Freq.

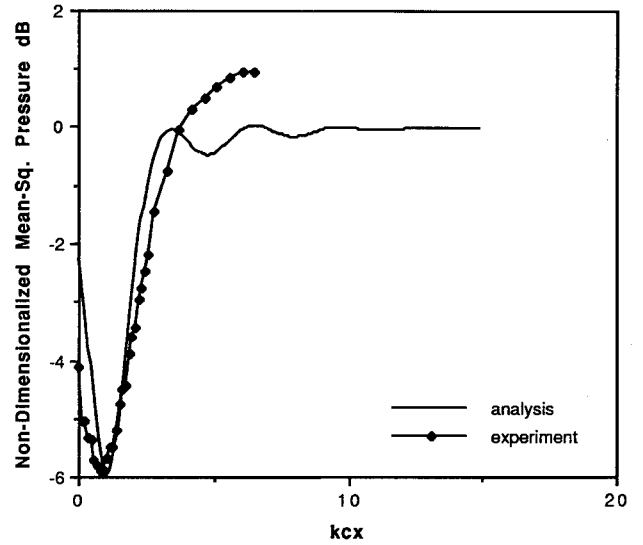


Fig. 7 Comparison of theoretically computed and experimentally measured nondimensionalized mean-square pressure in dB vs $k_c x$: 2000-Hz center frequency, $1/3$ octave band.

easy to implement. This involves changing k_c from a constant, evaluated at the center frequency, to a k , a variable, and integrating the expression over the band Δk .

Comparisons between theoretically calculated results and experimentally measured data are shown in Figs. 7–9 for three different center frequencies: 2000, 3250, and 4000 Hz, respectively. The impedance of the foam is different at each center frequency. At 2000 Hz, the normalized resistance (\bar{r}_b) is 1.17 and the normalized reactance (\bar{x}_b) is -0.84 . These impedance characteristics correspond to an equivalent random incidence absorption coefficient α of 0.85. At 3250 Hz, $\bar{r}_b = 1.44$, $\bar{x}_b = 0.15$, and the corresponding $\alpha = 0.95$. At 4000 Hz, $\bar{r}_b = 1.47$, $\bar{x}_b = 0.64$, and the equivalent value for α is 0.91.

The theoretical results are for the three-dimensional case with bandwidth included. These three examples are plotted for a $1/3$ octave bandwidth. The experimental data were taken as an extension of an experiment that was used to validate the asymptotic modal analysis method for a rectangular acoustic

cavity with rigid walls. The apparatus and details of the experiment are described in Ref. 18. However, the original apparatus was modified by placing an open-cell acoustic foam on one wall of the cavity. The experimental data were taken by moving a microphone into the cavity from the foam-covered wall and recording the measured sound pressure levels.

The theoretical curves show clear asymptotic behavior, whereas the experimental curves settle down less rapidly. The physical system in the experiment was a three-dimensional enclosure with rigid walls. Provided that the rigid walls were in the far field of the microphone, so that their intensification zones were not penetrated by the microphone, the experiment should be analogous to the theoretical model. Although this condition was satisfied, it appears from the experimental data that the interior of the cavity was not uniform. Previous work, both analytical^{1,2} and experimental¹⁸ have shown that, when

Absorption Results: 3250 Hz Center Freq.

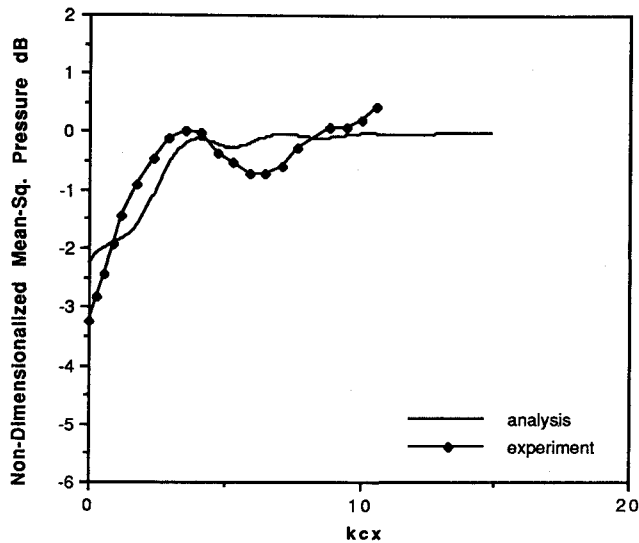


Fig. 8 Comparison of theoretically computed and experimentally measured nondimensionalized mean-square pressure in dB vs $k_c x$: 3250-Hz center frequency, $1/3$ octave band.

Absorption Results: 4000 Hz Center Freq.

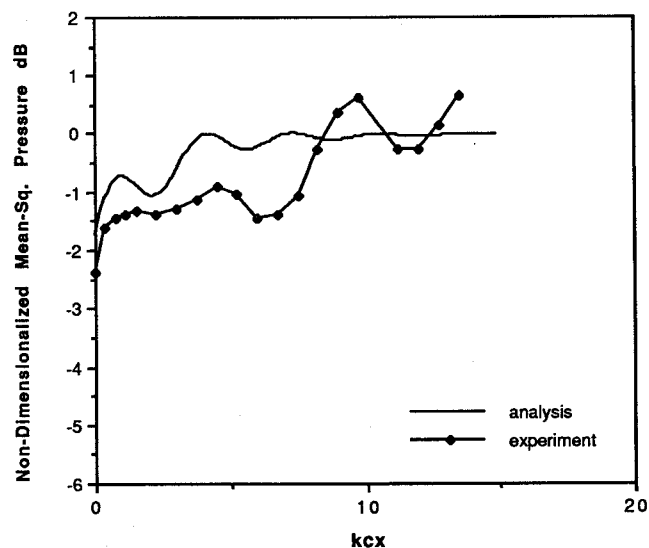


Fig. 9 Comparison of theoretically computed and experimentally measured nondimensionalized mean-square pressure in dB vs $k_c x$: 4000-Hz center frequency, $1/3$ octave band.

the damping in the cavity is small, the cavity interior is uniform except in the intensification regions. Covering one wall with the absorptive foam apparently added enough damping to prevent the interior sound pressure levels from becoming uniform.

The wall impedance dramatically changes the character of the intensification region. In fact, as Figs. 7-9 show, the sound pressure levels at the wall can be reduced well below the interior levels if the wall is sufficiently absorptive. Despite the discrepancies away from the wall, the curves show reasonable qualitative agreement between the analytical and experimental results near the wall, as is consistent with the local nature of the intensification process.

Bandwidth Effect

The key parameter in all of the previous studies was the bandwidth to center frequency ratio f_b/f_c . In order to isolate

the contribution of the bandwidth from that of the center frequency, a Taylor series expansion was performed. For example, Eq. (6) for the two-dimensional waves in the intensification zone is a double integral in k and α . It can be written as a Taylor series expansion about the center frequency wave number k_c as follows:

$$\begin{aligned} \int_0^{\pi/2} \int_{k_l}^{k_u} F(k, \alpha) dk d\alpha &= \int_0^{\pi/2} \int_{k_l}^{k_u} F(k_c, \alpha) dk d\alpha \\ &+ \int_0^{\pi/2} \int_{k_l}^{k_u} \left. \frac{\partial F(k, \alpha)}{\partial k} \right|_{k_c} (k - k_c) dk d\alpha \\ &+ \int_0^{\pi/2} \int_{k_l}^{k_u} \left. \frac{\partial^2 F(k, \alpha)}{\partial k^2} \right|_{k_c} \frac{(k - k_c)^2}{2!} dk d\alpha + \dots \end{aligned} \quad (9)$$

Using the arithmetic definition of center frequency, i.e., $k_c = (k_u + k_l)/2$, the integrals of odd powers of $(k - k_c)$ will equal zero, leaving only the integrals of even powers of bandwidth. Nondimensionalizing introduces a factor of bandwidth in the denominator. Therefore, the resulting function will consist of a term that is dependent only on center frequency plus higher-order terms that contain bandwidth squared and the higher even powers of bandwidth.

An illustrative example, which can be solved in closed form, is the intensification in a corner approaching along an edge, where the motion of the wall is such that the displacement is relatively constant (white noise) in the bandwidth. For this case, the nondimensional mean-square pressure expression is

$$\frac{\bar{p}^2}{(\bar{p}^2)} = \frac{\iiint_{k, \phi, \theta} \cos^2(kz \cos \theta) k \sin \theta d\theta d\phi dk}{\frac{1}{8} \iiint_{k, \phi, \theta} k \sin \theta d\theta d\phi dk} \quad (10)$$

This equation differs from Eq. (8) by a factor of k^2 in the integrals, since Eq. (8) is for the case where the white noise assumption is applied to the acceleration of the moving wall, rather than its displacement. The z axis is taken as the edge along which the intensification is studied. This expression has the closed-form solution:

$$\frac{\bar{p}^2}{(\bar{p}^2)} = \frac{4 + 2 \sin(2k_c z) \sin[(k_b/k_c)k_c z]}{(k_c z)^2 (k_b/k_c)} \quad (11)$$

All center frequency subscripts here refer to the arithmetic center frequency. Alternatively, the Taylor series expansion procedure outlined in Eq. (9) and performed on Eq. 10 yields

$$\begin{aligned} \frac{\bar{p}^2}{(\bar{p}^2)} &= 4 + 4 \frac{\sin(2k_c z)}{2k_c z} - \frac{1}{3} \left(\frac{k_b}{k_c} \right)^2 (k_c z) \sin(2k_c z) \\ &+ \text{higher order terms} \end{aligned} \quad (12)$$

Expanding the sine $(k_b/k_c)k_c z$ term in Eq. (11) in a Taylor series about the center frequency wave number produces an identical result. This approximate solution is only valid in the region where the sine function is closely approximated by a two-term Taylor series. For greater accuracy, the solution would have to include higher-order bandwidth to center frequency ratio terms. The two-term Taylor series for sine is only valid up to arguments approximately equal to 1.25. Therefore, in this example, the combination $(k_b/k_c)(k_c z)$ must be ≤ 1.25 , or conservatively ≤ 1.0 , which means that $k_c z \leq 1/(k_b/k_c)$ for the approximate solution to be accurate. Typically, intensification occurs close to the wall, edge, or corner where the

"CF Curve" - No Bandwidth Effect

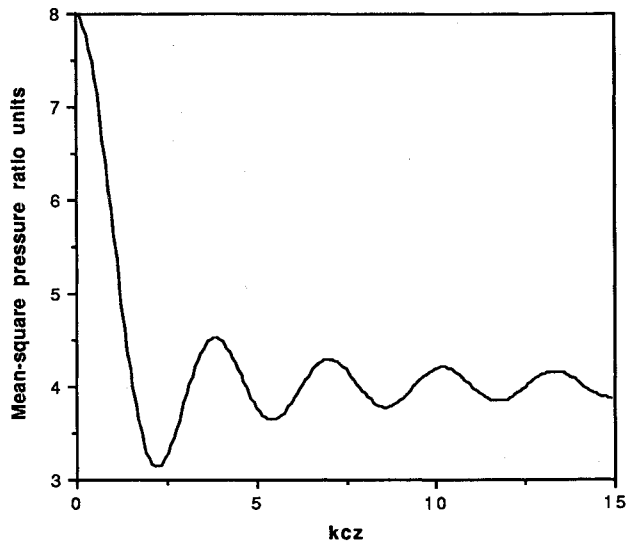


Fig. 10 CF curve that is dependent upon $k_c z$ only: nondimensionalized mean-square pressure ratio vs $k_c z$ for the example problem.

"Correction Curve"

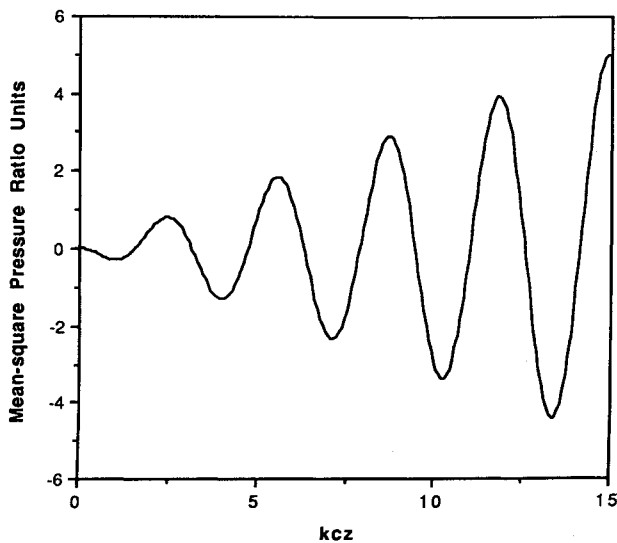


Fig. 11 Correction curve that is to be multiplied by f_b/f_c ratio squared: this curve by itself is also independent of bandwidth.

values of $k_c x$, $k_c y$, or $k_c z$ are small. In fact, usually, $k_c x$, $k_c y$, and/or $k_c z \leq 2\pi/3$. Therefore, in most cases, the two-term solution should be sufficient. For a $1/3$ octave band, for example f_b/f_c is 0.23, which satisfies the requirement that $k_c z < 1/(k_b/k_c)$.

Since the bandwidth correction is second order in bandwidth, the mean-square pressure can be approximated by a simple curve that is dependent on center frequency (CF) only for small bandwidths. This curve (the CF curve) for the current example problem is plotted in Fig. 10. It is a function of $k_c x$ alone, and is independent of bandwidth. The effects of increasing bandwidth can be taken into account by adding another function of center frequency that has been multiplied by the ratio $(f_b/f_c)^2$. This function, called the correction curve, is shown in Fig. 11 [before multiplication by $(f_b/f_c)^2$] for this example.

In Fig. 12, the correction curve has been multiplied by $(0.23)^2$ and then added to the CF curve. The results are expected to be accurate up to $k_c z$ around 4.0, as explained

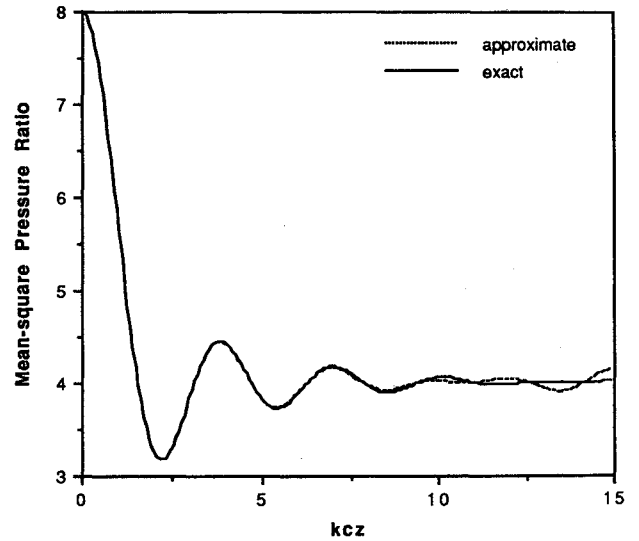
Exact Vs. Approximate - $f_b/f_c = .23$ 

Fig. 12 Comparison of exact solution vs the approximate solution consisting of CF curve + $(f_b/f_c)^2$ correction curve, for $f_b/f_c = 0.23$ ($1/3$ octave band).

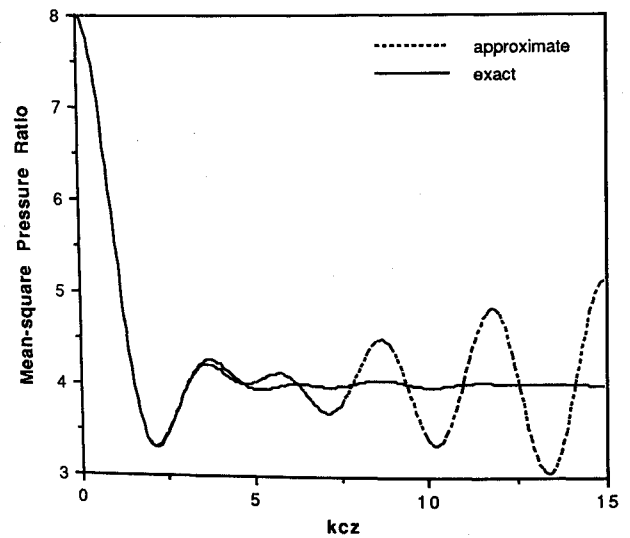
Exact Vs. Approximate - $f_b/f_c = .5$ 

Fig. 13 Comparison of exact solution vs the approximate solution consisting of CF curve + $(f_b/f_c)^2$ correction curve, for $f_b/f_c = 0.500$.

earlier. However, the exact solution and the approximate solution agree with each other well beyond 4.0. In Fig. 13, a similar comparison between the approximate solution and the exact solution is made for $f_b/f_c = 0.5$. Here, good agreement is expected up to 2.0. Once again, the agreement actually extends beyond that predicted. From the plot, it is also easy to see that the approximate solution fails for large $k_c z$.

Conclusions

In previous work, asymptotic modal analysis was used to predict interior sound pressure levels in a rectangular acoustic cavity. Local response peaks in sound pressure level were found at the boundaries; otherwise, the interior levels were nearly constant. In the present work, the spatial variation of sound pressure level between the boundary and the uniform interior was studied, i.e., the intensification zone.

It was found that using such AMA techniques as treating the discrete summation as an integration, and evaluating certain parameters at the center frequency, etc., provides accu-

rate results even when the number of modes is relatively few. In addition, the AMA formulation allows estimation of the mean-square pressure ratio as a function of nondimensionalized distance into the cavity, without knowing the cavity dimensions. The family parameter for the curves of nondimensionalized mean-square pressure vs nondimensionalized distance (distance multiplied by the center frequency wave number) is the bandwidth to center frequency ratio f_b/f_c . Plots of one-, two-, and three-dimensional intensification zones have shown that the dependence on f_b/f_c is less important as the number of modal dimensions increases, i.e., the effect is least important in the three-dimensional case.

The bandwidth dependence was separated from the center frequency dependence through a Taylor series expansion about the center frequency wave number, which was performed on the expression for mean-square pressure. As a result, the mean-square pressure can be expressed as a function of center frequency plus terms that are of order bandwidth to center frequency ratio squared, and higher (even powers). Therefore, if the bandwidth to center frequency ratio is sufficiently small, the expression can be simplified. If several bandwidth to center frequency ratios are to be considered, their effects can be added on as corrections that are of order $(f_b/f_c)^2$.

The intensification zones were also analyzed as local problems consisting of an infinite number of oblique incidence sound waves impinging upon a rigid or an absorptive surface. The result for the spatial average of the sound pressure levels in the rigid wall case was identical to that obtained from the AMA methods. The result for the absorptive wall was found to contain the rigid wall result as well as additional terms that contain the impedance information. The shape of the intensification zone is strongly affected by the choice of wall impedance and can be remarkably different from that near a rigid wall. In particular, minimum rather than maximum levels may occur in this zone. The absorptive wall analytical result was compared with experimental results and found to agree qualitatively near the wall.

The results of this work provide physical insight into the intensification zone behavior in acoustic cavities by providing analytical expressions that describe the sound field in terms of universal components that show the importance of various parameters. The analytical techniques that were used here provide efficient and accurate methods for predicting sound pressure levels in rooms with intensification zones.

Acknowledgments

This work was supported by the Structural Acoustics Branch of NASA Langley Research Center through Grant NAG-1-709 and NASA Graduate Student Researchers Program Fellowship NGT-50342. The authors also wish to thank Donald Bliss of Duke University for his comments, suggestions, and stimulating discussions regarding this work.

References

- ¹Kubota, Y., Dionne, H. D., and Dowell, E. H., "Asymptotic Modal Analysis and Statistical Energy Analysis of an Acoustic Cavity," *Journal of Vibration, Acoustics, Stress and Reliability in Design*, Vol. 110, No. 3, 1988, pp. 371-376.
- ²Peretti, L. F., and Dowell, E. H., "Asymptotic Modal Analysis of a Rectangular Acoustic Cavity Excited by Wall Vibration," *AIAA Journal*, Vol. 30, No. 5, pp. 1191-1198.
- ³Pierce, A. D., "Room Acoustics," *Acoustics: An Introduction to Its Physical Principles and Applications*, Acoustical Society of America, Woodbury, NY, 1989, Chap. 6.
- ⁴Kinsler, L. E., and Frey, A. R., "Architectural Acoustics," *Fundamentals of Acoustics*, 2nd Ed., Wiley, New York, 1962, Chap. 14.
- ⁵Morse, P. M., and Ingard, K. U., "Room Acoustics," *Theoretical Acoustics*, McGraw-Hill, New York, 1968, Chap. 9.
- ⁶Crandall, S. H., "Random Vibration of One- and Two-Dimensional Structures," *Developments in Statistics*, Vol. 2, edited by P. R. Krishnaiah, Academic, New York, 1979, pp. 1-82.
- ⁷Itao, K., and Crandall, S. H., "Wide-Band Random Vibration of Circular Plates," *Journal of Mechanical Design*, Vol. 100, No. 4, 1978, pp. 690-695.
- ⁸Crandall, S. H., and Kulvets, A. P., "Source Correlation Effects on Structural Response," *Application of Statistics*, edited by P. R. Krishnaiah, North-Holland, New York, 1977, pp. 168-182.
- ⁹Kubota, Y., and Dowell, E. H., "Experimental Investigation of Asymptotic Modal Analysis for a Rectangular Plate," *Journal of Sound and Vibration*, Vol. 106, No. 2, 1986, pp. 203-216.
- ¹⁰Waterhouse, R. V., "Interference Patterns in Reverberant Sound Fields," *Journal of the Acoustical Society of America*, Vol. 27, No. 2, 1955, pp. 247-258.
- ¹¹Chu, W. T., "Eigenmode Analysis of the Interference Patterns in Reverberant Sound Fields," *Journal of the Acoustical Society of America*, Vol. 68, No. 1, 1980, pp. 184-190.
- ¹²Chu, W. T., "Comments on the Coherent and Incoherent Nature of a Reverberant Sound Field," *Journal of the Acoustical Society of America*, Vol. 69, No. 6, 1981, pp. 1710-1715.
- ¹³Tohyama, M., and Suzuki, A., "Space Variances in the Mean-Square Pressure at the Boundaries of a Rectangular Reverberation Room," *Journal of the Acoustical Society of America*, Vol. 80, No. 3, 1986, pp. 828-832.
- ¹⁴Waterhouse, R. V., "Noise Measurement in Reverberant Rooms," *Journal of the Acoustical Society of America*, Vol. 54, No. 4, 1973, pp. 931-934.
- ¹⁵Waterhouse, R. V., and Cook, R. K., "Diffuse Sound Fields: Eigenmode and Freewave Models," *Journal of the Acoustical Society of America*, Vol. 59, No. 3, 1976, pp. 576-581.
- ¹⁶Waterhouse, R. V., and Cook, R. K., "Interference Patterns in Reverberant Sound Fields. II," *Journal of the Acoustical Society of America*, Vol. 37, No. 3, 1965, pp. 424-428.
- ¹⁷Dowell, E. H., Gorman, G. F., III, and Smith, D. A., "Acoustoelasticity: General Theory, Acoustic Natural Modes and Forced Response to Sinusoidal Excitation, Including Comparisons with Experiment," *Journal of Sound and Vibration*, Vol. 52, No. 4, 1977, pp. 519-542.
- ¹⁸Peretti, L. F., and Dowell, E. H., "Experimental Verification of the Asymptotic Modal Analysis Method as Applied to a Rectangular Acoustic Cavity Excited by Structural Vibration," *Journal of Vibrations and Acoustics* (to be published).